Role of further-neighbor interactions in modulating the critical behavior of the Ising model with frustration

R. M. Liu,[1] W. Z. Zhuo,[1] S. Dong,[2] X. B. Lu,[1] X. S. Gao,[1] M. H. Qin,[1,*] and J.-M. Liu[1,3,†]

[1]*Institute for Advanced Materials and Guangdong Provincial Key Laboratory of Quantum Engineering and Quantum Materials, South China Normal University, Guangzhou 510006, China*

[2]*Department of Physics, Southeast University, Nanjing 211189, China*

[3]*Laboratory of Solid State Microstructures, Nanjing University, Nanjing 210093, China*

(Received 24 November 2015; revised manuscript received 22 January 2016; published 8 March 2016)

In this work, we investigate the phase transitions and critical behaviors of the frustrated J_1-J_2-J_3 Ising model on the square lattice using Monte Carlo simulations, and particular attention goes to the effect of the second-next-nearest-neighbor interaction J_3 on the phase transition from a disordered state to the single stripe antiferromagnetic state. A continuous Ashkin-Teller–like transition behavior in a certain range of J_3 is identified, while the four-state Potts-critical end point $[J_3/J_1]_C$ is estimated based on the analytic method reported in earlier work [Jin, Sen, and Sandvik, Phys. Rev. Lett. **108**, 045702 (2012)]. It is suggested that the interaction J_3 can tune the transition temperature and in turn modulate the critical behaviors of the frustrated model. Furthermore, it is revealed that an antiferromagnetic J_3 can stabilize the staggered dimer state via a phase transition of strong first-order character.

DOI: 10.1103/PhysRevE.93.032114

I. INTRODUCTION

Symmetry breaking at a thermal phase transition decides orders. For example, the spontaneous breaking of Z_2 symmetry in the well-known frustrated two-dimensional (2D) antiferromagnetic (AFM) J_1-J_2 model on the square lattice leads to the Néel state [Ising AFM state, Fig. 1(a)] for $J_2/J_1 < 1/2$ [1–4]. The phase transition between the Ising AFM state and a disordered state belongs to the 2D Ising universality class. Furthermore, for $J_2/J_1 > 1/2$, a Z_4 symmetry can be broken below the critical temperature ($T \leqslant T_C$), resulting in the single stripe AFM state [Fig. 1(b)] [5]. More interestingly, the nature of this phase transition cannot be directly obtained from the symmetry of the order parameter, and different phase-transition scenarios apply depending on the value of J_2/J_1, as will be introduced below [6].

In the 1980s, it was generally believed that the transition to the single stripe order is continuous but with varying critical exponents for different J_2/J_1 [7–10]. However, this point of view was suspected by the mean-field calculation in 1993 which found a first-order transition for a certain region of J_2/J_1 [11]. Subsequently, the existence of the first-order transition was further confirmed by Monte Carlo (MC) simulations [12–14]. In particular, the transition for $1/2 < J_2/J_1 \leqslant 1$ was suggested to be of weak first-order based on a double-peak structure in energy histograms. Furthermore, it was suggested that the transition for large $J_2/J_1 > 1$ is continuous with the Ashkin-Teller (AT) criticality [14,15].

More recently, the nature of the stripe phase transition in the J_1-J_2 model was clearly elucidated by employing a combination of MC simulations and analytical methods, and the transition point between the two scenarios (first-order and AT-like transitions) was estimated to be at a value of $J_2/|J_1| \approx 0.67$ [6,16]. The phase transition at this critical point is in the four-state Potts universality class, and those for $1/2 < J_2/J_1 < 0.67$ are of weak first order [17]. More interestingly, a pseudo-first-order behavior was uncovered for $0.67 \leqslant J_2/|J_1| \leqslant 1$, similar to that of the AT model in a certain parameter region. It was demonstrated that some signatures were not sufficient as proofs of first-order transition, leading to the former overestimation of the region of first-order character in the J_1-J_2 model. This behavior was also verified by the large-scale MC simulations which show that the first-order signals in the energy histograms vanish at large system sizes $L \sim 2000$ at $J_2/J_1 = 0.8$ [18].

While the phase transitions and critical behaviors of the frustrated J_1-J_2 model are being progressively uncovered [as summarized in Fig. 1(c)], studies proceed in the models with further-neighboring interactions. The study of the role of further-neighboring interactions on the critical behaviors becomes important from the following two viewpoints. On one hand, the single stripe order and various transition behaviors have been experimentally reported in most of the iron-based superconductors. The exchange interaction paths in relevant materials are very complicated. Further-neighboring interactions may be available and play an important role in determining the magnetic properties due to the spin frustration [19]. For example, a nonzero coupling J_3 between the third-nearest neighbors is suggested to be important for the magnetic properties in iron chalcogenides such as FeTe [20]. On the other hand, this study can also contribute to the development of statistical mechanics and solid-state physics. For example, more interesting AFM orders such as staggered dimer and double stripe states [shown in Figs. 2(a) and 2(b), respectively] can be stabilized by an AFM J_3, and the transition behaviors are also very attractive. Furthermore, the interesting scenarios for the single stripe phase transition in the J_1-J_2 model discussed above promote the development of phase-transition theory. However, there are still open questions such as whether these scenarios hold true for the model

*qinmh@scnu.edu.cn
†liujm@nju.edu.cn

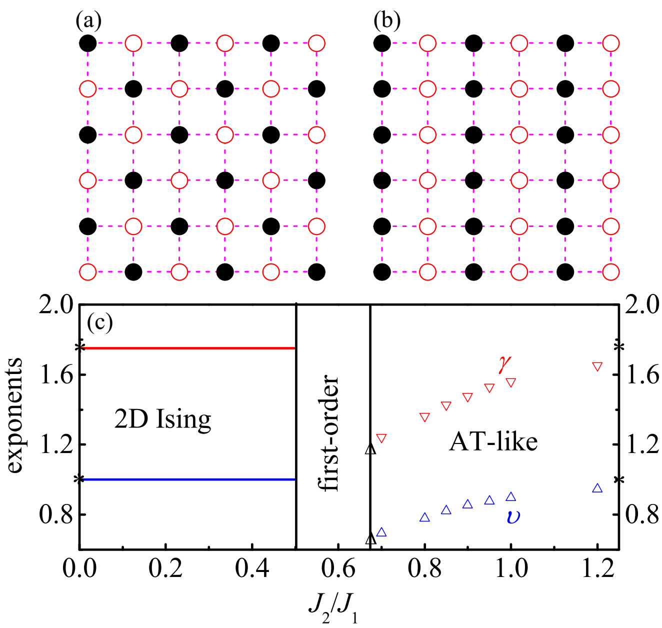

FIG. 1. Spin configurations in the (a) Néel state, and (b) single stripe state. Solid and empty circles represent the up-spins and the down-spins, respectively. (c) The critical behaviors of the frustrated J_1-J_2 model on the square lattice. The Potts values (black triangles) and the Ising values (black stars) are also given, and these critical exponents for $J_2/J_1 > 0.67$ are reproduced from Ref. [18].

with further-neighboring interactions, and how the critical behaviors are determined. To some extent, these questions are related to the universality of the phase transition, and definitely deserve to be checked in detail.

In this work, we study the frustrated J_1-J_2-J_3 Ising model on the 2D square lattice to unveil the role of J_3 in modulating the critical behaviors. The MC simulated results show that the critical exponents of the single stripe AFM transition vary with the increasing magnitude of ferromagnetic (FM) J_3 (at $J_2/J_1 = 0.8$, for example). Similarly, a pseudo-first-order behavior is observed for small AFM J_3, and the four-state Potts-critical end point is also reasonably estimated. Furthermore, the transition from a disorder state to the staggered dimer state is investigated, which exhibits a strong first-order behavior.

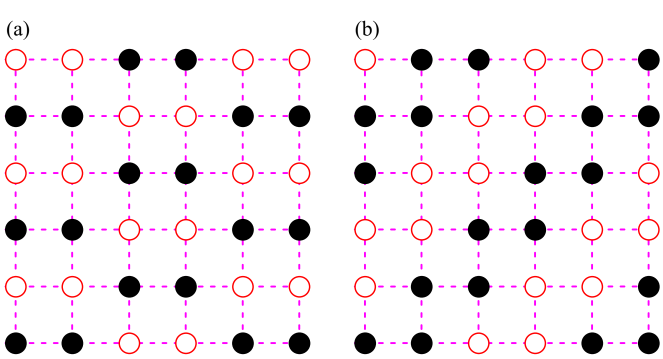

FIG. 2. Spin configurations in the (a) staggered dimer state, and (b) double stripe state. Solid and empty circles represent the up-spins and the down-spins, respectively.

The rest of this paper is organized as follows. In Sec. II the model and the simulation method will be presented and described. Section III is dedicated to the simulation results and discussion. The Conclusion is presented in Sec. IV.

II. MODEL AND METHOD

The model Hamiltonian can be written as

$$H = J_1 \sum_{\langle ij\rangle_1} S_i S_j + J_2 \sum_{\langle ij\rangle_2} S_i S_j + J_3 \sum_{\langle ij\rangle_3} S_i S_j, \tag{1}$$

where $J_1 = 1$ is the unit of energy, $S_i = \pm 1$ is the Ising spin with unit length on site i, and $\langle ij\rangle_n$ denotes the summations over all the nth-nearest neighbors with coupling J_n.

For a description of the single stripe order, the order parameter m_s can be defined as

$$m_s^2 = m_x^2 + m_y^2, \tag{2}$$

with

$$m_{x,y} = \frac{1}{N} \sum_i (-1)^{i_{x,y}} S_i, \tag{3}$$

where (i_x, i_y) are the coordinates of site i on a $N = L \times L (24 \leqslant L \leqslant 256)$ periodic lattice. In order to understand the nature of the phase transition, we calculate the Binder cumulant U_s:

$$U_s = 2\left(1 - \frac{1}{2}\frac{\langle m_s^4\rangle}{\langle m_s^2\rangle^2}\right), \tag{4}$$

and susceptibility χ_s:

$$\chi_s = N\left(\langle m_s^2\rangle - \langle m_s\rangle^2\right)/T, \tag{5}$$

where $\langle \ldots \rangle$ is the ensemble average.

The staggered dimer state is eightfold degenerate, and the order parameter m_d can be similarly defined as

$$m_d^2 = \sum_{k=1}^{4} m_k^2, \tag{6}$$

with

$$m_k = \sum_i A_k(i_x, i_y) S_i, \tag{7}$$

where the value of $A_k(i_x, i_y)$ depends on the coordinates of site i and the spin configurations of the ground states. Take the configuration shown in Fig. 2(a) as an example, $A(i_x, i_y) = 1$ for up-spins, and $A_k(i_x, i_y) = -1$ for down-spins. Furthermore, the Binder cumulant U_d is also calculated.

Our simulation is performed using the standard Metropolis algorithm and the parallel tempering algorithm [21,22]. We take an exchange sampling after every ten standard MC steps. The initial 5×10^5 MC steps are discarded for equilibrium consideration and another 5×10^5 MC steps are retained for statistic averaging of the simulation. Generally, we choose $J_2 = 0.8$ and change J_3 in computation in studying the single stripe phase transition. It is noted that J_3 has no effect on the competition between the stripe state and the Ising AFM state [23], and the former state occupies the whole studied J_3 region ($J_3 < 0.15$). Furthermore, it will be checked later that the choice of J_2 never affects our conclusion. On the other

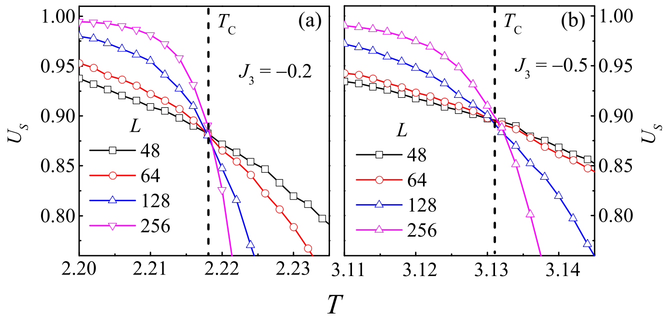

FIG. 3. Binder cumulant U_s as a function of T for different L at $J_2 = 0.8$ at (a) $J_3 = -0.2$ and (b) $J_3 = -0.5$.

hand, $J_2 = 0.5$ is selected to study the phase transition to the staggered dimer state.

III. SIMULATION RESULTS AND DISCUSSION

A. Varying critical exponents with ferromagnetic J_3

First, we study the effect of FM J_3 on the phase transition and its critical behaviors. Figures 3(a) and 3(b) show the simulated U_s as a function of T at $J_3 = -0.2$ and -0.5 for different L. For continuous phase transitions, the Binder cumulant for different L usually crosses at the critical point. From the common well-defined crossing points, we estimate $T_C = 2.218(5)$ at $J_3 = -0.2$ and $T_C = 3.131(5)$ at $J_3 = -0.5$. In fact, it is rather clear that the single stripe order can be further favored by a FM J_3, and the transition point shifts toward high T when the magnitude of J_3 is increased, as shown in our simulations.

In the AT model, the critical exponents ν and γ vary with the magnitude of the frustration, while the ratio of $\gamma/\nu = 7/4$ keeps constant [24]. This critical behavior is also observed in our simulations of the J_1-J_2-J_3 Ising model, as shown in Fig. 4. The critical exponents are estimated based on the standard finite-size scaling fact that the slope of U vs T at $T_C, dU/dT(T_C)$, is proportional to $L^{1/\nu}$, and $\chi_{\max}$ is proportional to $L^{\gamma/\nu}$. It is clearly shown that ν increases with the increasing magnitude of J_3 and/or T_C. For example, $\nu = 0.83(3)$ at $J_3 = -0.2$ and $\nu = 0.88(5)$ at $J_3 = -0.5$ are estimated, as shown in Fig. 4(a). Furthermore, the roughly constant $\gamma/\nu = 7/4$ is obtained for every FM J_3 [Fig. 4(b)], within the limits of acceptable error (at most, $\sim$1.8%), demonstrating an AT-like behavior. In Fig. 5, we plot

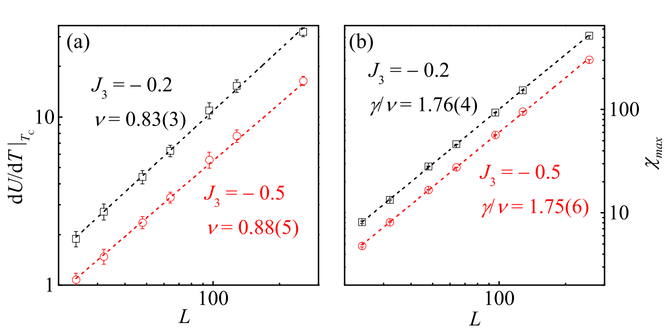

FIG. 4. Log-log plot of (a) $dU/dT(T_C)$, and (b) $\chi_{\max}$ for various L at $J_3 = -0.2$ and $J_3 = -0.5$ for $J_2 = 0.8$.

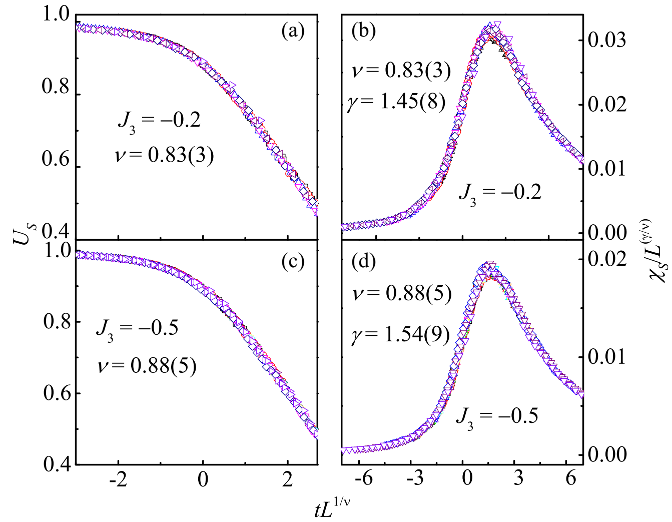

FIG. 5. A scaling plot of U_s (a) and (c) and χ_s (b) and (d) at $J_3 = -0.2$ (a) and (b) and $J_3 = -0.5$ (c) and (d) at $J_2 = 0.8$.

the simulated U_s and χ_s in the scaling form: $U_s = f(tL^{1/\nu})$, and $\chi_s = L^{\gamma/\nu}g(tL^{1/\nu})$, with $t = (T{-}T_C)/T_C$, at $J_3 = -0.2$ and -0.5. It is confirmed that the single stripe phase transition at $T_C = 2.218(5)$ for $J_3 = -0.2$ is with the critical exponents $\nu = 0.83(3)$ and $\gamma = 1.45(8)$, and that at $T_C = 3.131(5)$ for $J_3 = -0.5$ is with $\nu = 0.88(5)$ and $\gamma = 1.54(9)$.

B. Location of the Potts-critical end point

If the continuous single stripe phase transition in the J_1-J_2-J_3 model can be mapped to the critical line of the AT model, a four-state Potts-critical end point is expected at an AFM J_3 which destabilizes this order and diminishes T_C [25]. In fact, pseudo-first-order or weak-first-order behavior is also observed at small AFM J_3 for intermediate L. Figure 6 gives the U_s as a function of T for various L at $J_3 = 0.05$ and 0.15. A negative peak is developed for $L = 128$ at $J_3 = 0.05$ and grows as L further increases, indicating a pseudo- or weak-first-order transition behavior, as clearly shown in Fig. 6(a) [26]. Furthermore, the system size needed to stabilize a negative peak is decreased when J_3 is increased [for example, $L = 24$ at $J_3 = 0.15$, as shown in Fig. 6(b)], demonstrating an enhancing discontinuity of m_s.

It is noted that the negative cumulant peak is not a sufficient proof for the first-order transition because such a peak can

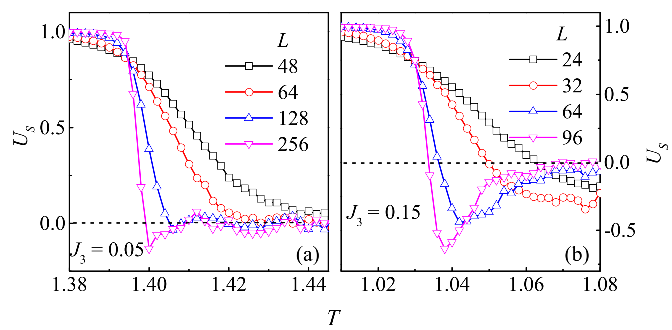

FIG. 6. Binder cumulant U_s as a function of T for different L at $J_2 = 0.8$ at (a) $J_3 = 0.05$ and (b) $J_3 = 0.15$.

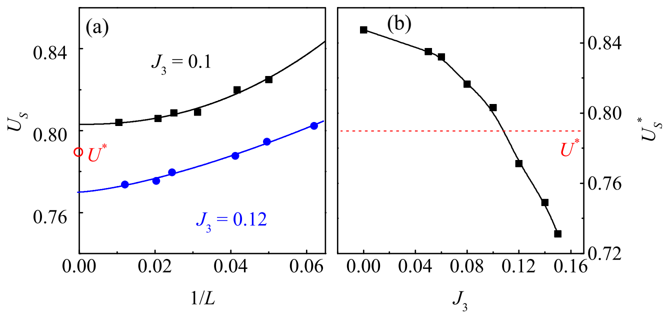

FIG. 7. (a) Binder cumulant crossing points U_s for $(L, 2L)$ system pairs and the extrapolation to $L = \infty$, and (b) U_s^* of the J_1-J_2-J_3 model for various J_3 at $J_2 = 0.8$ compared with that of the four-state Potts model.

appear also for continuous transitions in spin models such as the four-state Potts and AT models [6]. However, the Binder crossing value U^* is normally universal and may characterize the universality class of the phase transition. Thus, following earlier works, the four-state Potts-critical end point of the AT line in the J_1-J_2-J_3 model can be reasonably estimated based on the analysis of the universality of the Binder cumulants ($U^* \approx 0.79$ for the four-state Potts model). Figure 7(a) shows the Binder cumulant crossing points for pairs $(L, 2L)$ and $L = \infty$ extrapolated U_s^* for various J_3. It is clearly shown that U_s^* decreases with increasing J_3. Finally, critical $[J_3/J_1]_C = 0.11 \pm 0.01$ for $J_2/J_1 = 0.8$ is obtained by comparing $U_s^*(J_3)$ with U^* for the four-state Potts model, as shown in Fig. 7(b).

C. Single stripe phase-transition behaviors and discussion

The simulated results of the single stripe phase transition for $J_2 = 0.8$ are summarized in Fig. 8(a). The critical temperature for $J_3 \geqslant 0.05$ is estimated from the position of the peak of the $\chi(T)$ curve for the largest L [27]. The phase diagram exhibits two regions with different transition behaviors, similar to that of the J_1-J_2 model. In detail, an AT-like behavior is observed for $J_3 \leqslant 0.11$, in which ν and γ increase continuously from those of the four-state Potts model to those of the 2D Ising model, respectively. More interestingly, our simulations also show a close dependence of the values of ν and γ on the transition point T_C for a fixed J_1, indicating that this phenomenon may be universal in the single stripe phase transitions in different models. In fact, similar behavior has been observed for other values of J_2. Specifically, Fig. 8(b) gives the estimated Potts-critical end points $[J_3/J_1]_C$ for different J_2. $[J_3/J_1]_C$ shifts toward the high J_3 side as J_2 increases, while the transition point T_C at $[J_3/J_1]_C$ is less affected. Furthermore, it is worth noting that the model has a symmetry $(J_1, J_2, J_3) \rightarrow (-J_1, J_2, J_3)$, and a FM J_1 would never affect our conclusion.

On one hand, the present work shows that the single stripe phase-transition behavior is also dependent on the exchange couplings between distant-neighboring spins. The phase-transition scenarios uncovered in the J_1-J_2 Ising model still hold true when the J_3 interaction is taken into account, further supporting the universality of these scenarios. In addition, it is suggested that the critical behavior may be likely dependent on the transition point which can be modulated through various methods. Of cause, additional proofs should be needed to double-check the universality of the transition pictures in some other frustrated spin models. On the other hand, the single stripe order as the ground state of most of the iron-based superconductors has drawn extensive attention in the past few years [28,29]. For example, the AFM phase transition in La-O-Fe-As is of first order, while that in $BaFe_2As_2$ is continuous [30]. To some extent, the transition scenarios uncovered in the frustrated Ising model on the square lattice may provide useful information in understanding the phase transitions in these materials, although some other degrees of freedom should be taken into account.

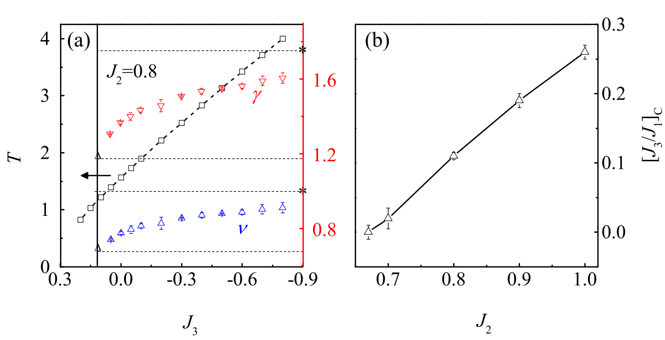

FIG. 8. (a) Phase diagram in the (J_3, T) parameter plane at $J_2 = 0.8$. The critical exponents ν and γ of the J_1-J_2-J_3 model, four-state Potts model (black triangles), and Ising model (black stars) are also given. (b) The estimated Potts-critical end points $[J_3/J_1]_C$ for various J_2.

D. Other orders in the phase diagram of the J_1-J_2-J_3 model

One may note that some other orders can be stabilized by AFM J_3 interaction [31,32]. In detail, Fig. 9 gives the ground-state phase diagram of the J_1-J_2-J_3 model which can be easily obtained by the mean-field method. It is clearly shown that the staggered dimer state is stabilized for AFM $J_3 < 0.5$ (yellow region), and the double stripe state or plaquette state occupies the $J_3 > 0.5$ region. Different from the fourfold degenerated single stripe state, the staggered dimer

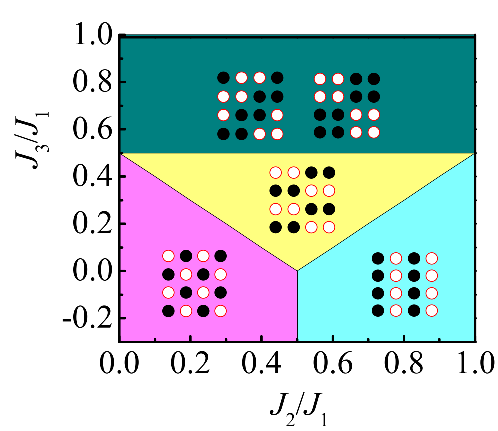

FIG. 9. Ground-state phase diagram in the (J_2, J_3) parameter plane. The spin configurations of these states are depicted. Solid and empty circles represent the up-spins and the down-spins, respectively.

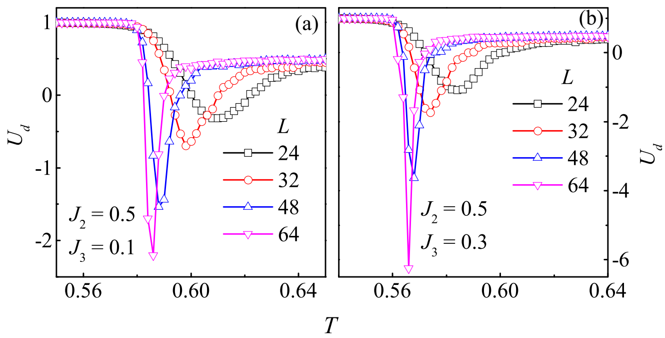

FIG. 10. Binder cumulant U_d as a function of T for different L at $J_2 = 0.5$ at (a) $J_3 = 0.1$ and (b) $J_3 = 0.3$.

state is eightfold degenerate. Thus, the phase transition to the staggered dimer state is expected to be of first order, similar to the transition in the eight-state Potts model. This viewpoint has been confirmed in our simulations. Figure 10(a) shows the calculated U_d as a function of T for various L at $J_3 = 0.1$ and $J_2 = 0.5$. Even for small $L = 24$, a clear negative peak can be developed, indicating a strong first-order transition behavior. Furthermore, for a fixed L, the peak of U_d grows with increasing J_3, as clearly shown in Fig. 10(b).

On the other hand, for the case of $J_3 > 0.5$, the double stripe state and the plaquette state are degenerated in the J_1-J_2-J_3 model on the square lattice. To study the transition behaviors of the double stripe state or the plaquette state, the degeneracy of these two states should be broken. To some extent, some other frustrated spin models such as the well-known Shastry-Sutherland model may be studied to investigate the phase transitions [33]. However, this topic is beyond the scope of this work, and will be left for our future work.

IV. CONCLUSION

In conclusion, the role of the third-nearest-neighbor interaction on the phase transitions and critical behaviors of the frustrated J_1-J_2-J_3 model on the square lattice is investigated using Monte Carlo simulations. In a certain range of J_3, the critical exponents of the continuous transition vary with the increase of the transition temperature, exhibiting an Ashkin-Teller–like behavior. In addition, the transition points at the Potts-critical end point estimated based on the analytic method are very similar for every J_2. Thus, this work suggests that the critical behaviors may be closely dependent on the transition point for a fixed J_1. Furthermore, a strong first-order behavior is confirmed for the transition to the staggered dimer state which is stabilized by an antiferromagnetic J_3.

ACKNOWLEDGMENTS

This work was supported by the Natural Science Foundation of China (Grants No. 51332007, No. 51322206, and No. 11274094), and the National Key Projects for Basic Research of China (Grants No. 2015CB921202 and No. 2015CB654602), and the International Science & Technology Cooperation Platform Program of Guangzhou (Grant No. 2014J4500016), and the Science and Technology Planning Project of Guangdong Province, China (Grant No. 2015B090927006).

[1] D. Friedan, Z. Qiu, and S. Shenker, Phys. Rev. Lett. **52**, 1575 (1984).
[2] H. T. Diep, *Frustrated Spin Systems* (World Scientific, Singapore, 2004).
[3] D. P. Landau and K. Binder, *A Guide to Monte Carlo Simulations in Statistical Physics* (Cambridge University Press, Cambridge, UK, 2008).
[4] H. Y. Wang, Phys. Rev. B **86**, 144411 (2012).
[5] M. P. Nightingale, Phys. Lett. A **59**, 486 (1977).
[6] S Jin, A. Sen, and A. W. Sandvik, Phys. Rev. Lett. **108**, 045702 (2012).
[7] R. H. Swendsen and S. Krinsky, Phys. Rev. Lett. **43**, 177 (1979).
[8] K. Binder and D. P. Landau, Phys. Rev. B **21**, 1941 (1980).
[9] J. Oitmaa, J. Phys. A **14**, 1159 (1981).
[10] D. P. Landau and K. Binder, Phys. Rev. B **31**, 5946 (1985).
[11] J. L. Morán-López, F. Aguilera-Granja, and J. M. Sanchez, Phys. Rev. B **48**, 3519 (1993).
[12] A. Malakis, P. Kalozoumis, and N. Tyraskis, Eur. Phys. J. B **50**, 63 (2006).
[13] A. Kalz, A. Honecker, S. Fuchs, and T. Pruschke, Eur. Phys. J. B **65**, 533 (2008).
[14] A. Kalz, A. Honecker, and M. Moliner, Phys. Rev. B **84**, 174407 (2011).
[15] J. Ashkin and E. Teller, Phys. Rev. **64**, 178 (1943).
[16] S. Jin, A. Sen, W. Guo, and A. W. Sandvik, Phys. Rev. B **87**, 144406 (2013).
[17] R. J. Baxter, J. Phys. C **6**, L445 (1973).
[18] A. Kalz and A. Honecker, Phys. Rev. B **86**, 134410 (2012).
[19] R. Yu and Q. M. Si, Phys. Rev. Lett. **115**, 116401 (2015).
[20] F. J. Ma, W. Ji, J. P. Hu, Z. Y. Lu, and T. Xiang, Phys. Rev. Lett. **102**, 177003 (2009).
[21] N. Metropolis, A. W. Rosenbluth, M. N. Rosenbluth, A. H. Teller, and E. Teller, J. Chem. Phys. **21**, 1087 (1953).
[22] K. Hukushima and K. Nemoto, J. Phys. Soc. Jpn. **65**, 1604 (1996).
[23] L. Huo, W. C. Huang, Z. B. Yan, X. T. Jia, X. S. Gao, M. H. Qin, and J.-M. Liu, J. Appl. Phys. **113**, 073908 (2013).
[24] R. J. Baxter, *Exactly Solved Models in Statistical Mechanics* (Academic Press, London, 1982).
[25] S. Wiseman and E. Domany, Phys. Rev. E **48**, 4080 (1993).
[26] K. Vollmayr, J. D. Reger, M. Scheucher, and K. Binder, Z. Phys. B **91**, 113 (1993).
[27] A. L. Wysocki, K. D. Belashchenko, and V. P. Antropov, Nat. Phys. **7**, 485 (2011).
[28] E. Dagotto, Rev. Mod. Phys. **85**, 849 (2013).
[29] M. H. Qin, S. Dong, H. B. Zhao, Y. Wang, J.-M. Liu, and Z. F. Ren, New J. Phys. **16**, 053027 (2014).
[30] P. C. Dai, Rev. Mod. Phys. **87**, 855 (2015).
[31] J. K. Glasbrenner, I. I. Mazin, H. O. Jeschke, P. J. Hirschfeld, R. M. Fernandes, and R. Valenti, Nat. Phys. **11**, 953 (2015).
[32] F. A. Kassan-Ogly, A. K. Murtazaev, A. K. Zhuravlev, M. K. Ramazanov, and A. I. Proshkin, J. Magn. Magn. Mater. **384**, 247 (2015).
[33] B. S. Shastry and B. Sutherland, Physica B+C **108**, 1069 (1981).